Available online at www.sciencedirect.com
ScienceDirect
Journal of Molecular Catalysis B: Enzymatic 55 (2008) 93–98
JOURNAL OF MOLECULAR CATALYSIS B: ENZYMATIC
www.elsevier.com/locate/molcatb

The direct electrochemistry behavior of Cyt *c* on the modified glassy carbon electrode by SBA-15 with a high-redox potential

Lin Zhu [a,b], Kunqi Wang [a,c], Tianhong Lu [a], Wei Xing [a,*], Jing Li [a], Xiangguang Yang [a]

[a] *Changchun Institute of Applied Chemistry, Chinese Academy of Sciences, Changchun 130022, PR China*
[b] *Graduate University of Chinese Academy of Sciences, Beijing 100049, PR China*
[c] *Changchun Institute of Technology, Changchun 130022, PR China*

Received 24 October 2007; received in revised form 29 January 2008; accepted 29 January 2008
Available online 15 February 2008

Abstract

It is discovered that SBA-15 (santa barbara amorphous) can provide the favorable microenvironments and optimal direct electron-transfer tunnels (DETT) of immobilizing cytochrome *c* (Cyt *c*) by the preferred orientation on it. A high-redox potential (254 mV vs. Ag/AgCl) was obtained on glassy carbon (GC) electrode modified by immobilizing Cyt *c* on rod-like SBA-15. With ultraviolet–visible (UV–vis), circular dichroism (CD), FTIR and cyclic voltammetry, it was demonstrated that immobilization made Cyt *c* exhibits stable and ideal electrochemical characteristics while the biological activity of immobilized Cyt *c* is retained as usual. The electrochemistry behavior at the modified GC electrode is surface-controlled quasi-reversible process with an enhanced electron-transfer rate constant of 2.20 s^{-1} because of the optimal DETT between Cyt *c* and SBA-15. It was also found that the modified GC electrode exhibited a predominant electrocatalytic activity for the reduction of hydrogen peroxide, which may open up a possibility for designing and fabricating enzyme electrodes with application potentials in biosensor and biofuel cells.

Keywords: SBA-15; Cytochrome *c*; Enzyme electrode; Biofuel cell

1. Introduction

SBA-15 is a mesoporous molecular sieve (MPS) with uniform tubular channels varying from 5 to 30 nm [1], which has attracted more and more researchers' attention in various branches of materials science and bioscience [2–5] since it was discovered in 1998 [6]. Its outstanding properties, such as highly ordered pore structures, large surface areas and huge pore volume, render it an ideal candidate as host for biomolecules. There have been a number of reports describing the use of SBA-15 to immobilize proteins or enzymes, such as catalase [7], lysozyme [8,9], HRP, subtilisin [4,10], myoglobin, trypsin, bovine serum albumin [11] and cytochrome *c* (Cyt *c*) [5,12,13]. Chaudhary et al. [14] indicated that the particle morphology along with the pore size and surface area are crucial constraint for the better accessibility of pore channel. The rod-like morphology appears to possess better accessibility to pore channels as the channels are arranged in a very straight and parallel manner. The MPS spheres are known to possess mesoporous channels that are arranged in either concentric rings or follow a non-aligned path, with high curvature, leading to lower levels of adsorption. Deere et al. [15–17] carried out a series of research for using MPS to immobilize proteins. They have shown, as have Yiu et al. [18], that the sizes of the pores of the MPS are crucial for adsorption onto the mesopore networks. In addition, the amount of protein adsorbed strongly decreased with increasing ionic strength. Vinu et al. [19] have studied the adsorption of Cyt *c* onto SBA-15 at different solution pH values. It has been found that the amount of Cyt *c* adsorbed on different adsorbents can be significantly changed by adjusting the solution pH. The maximum loading of Cyt *c* has been achieved near the isoelectric point of Cyt *c* (p*I* 9.8). Whereas in the case of the surface charges of the protein and the MPS are complementary, the adsorption to occur is facile [15].

Cyt *c* is a pseudo-spherical basic redox protein with relatively small size (2.6 nm × 3.2 nm × 3.0 nm) [20], which has been an active subject of immense biological investigation [15].

* Corresponding author at: State Key Laboratory of Electroanalytical Chemistry, Changchun Institute of Applied Chemistry, Chinese Academy of Sciences, 5625 Renmin Street, Changchun 130022, PR China. Tel.: +86 431 85262223; fax: +86 431 85685653.
E-mail address: xingwei@ciac.jl.cn (W. Xing).

1381-1177/$ – see front matter © 2008 Elsevier B.V. All rights reserved.
doi:10.1016/j.molcatb.2008.01.013

The active sites of Cyt *c*, heme groups, consist of a porphyrin ring, where a square planar complex is made by four pyrrole nitrogens co-ordinating to its central Fe atom [20]. The Cyt *c* molecule has a flat plane at one side where the heme group is exposed, which suggests that there is only one electroactive position of Cyt *c* molecules for DETT [21]. One more aspect of a protein, in addition to the overall structure, that contributes to its activity is the oxidation state of the central metal ion [14]. The switch between Fe^{3+} and Fe^{2+} is the main reaction of Cyt *c*. Because of its outer electronic structure, Fe^{3+} can exist in high-spin or low-spin states [20]. Cyt *c* was observed in both high-spin and low-spin states after being adsorbed on the MPS, in contrast to that in solution where the protein is predominantly in the low-spin state. The phenomenon may be due to the enhanced peroxidative activity of the adsorbed protein [15], resulting in an increase of the conformational transition energy from the oxidized form to the reduced one. Consequently, the redox potential shifts positively from its native redox potential (260 mV vs. NHE) [21,22]. However, there are few literatures reported the direct electrochemistry behavior of Cyt *c* on the electrode modified with SBA-15.

In the present research, a dramatic increase in electrochemical potential of Cyt *c* was obtained with the immobilization of SBA-15. It was discovered that the modified GC electrode showed the quasi-reversible electrochemistry behavior and enhanced electrocatalytic activity to the reduction of hydrogen peroxide. We interrupted that the enhancement in electrochemistry of the modification is relative to the isoelectric point (p*I*) and electrostatic interaction between Cyt *c* and SBA-15 in the immobilizing process, which provides a fast DETT by the optimum orientation of Cyt *c*.

2. Materials and methods

2.1. Materials

Horse heart cytochrome *c* (96%, Mw 12,384) was obtained from Sigma–Aldrich and used without purification. SBA-15 was synthesized according to the method reported in the literature [23]. The buffer solutions (0.1 M) were prepared from NaH_2PO_4 and Na_2HPO_4, and the pH was adjusted with HCl and KOH solutions. Other reagents were of analytical reagent grade. All solutions were prepared with triple-distilled water.

2.2. Apparatus and measurements

The electrochemical measurements were performed with an EG&G PAR (Princeton Applied Research) 273 potentiosat/galvanostat and a conventional three-electrode cell. The Ag/AgCl electrode and a Pt foil were used as the reference electrode and the auxiliary electrode, respectively. The GC electrode was used as substrate of the working electrode. Before the measurement, oxygen was purged from the solution by bubbling with highly purified nitrogen for 30 min and a nitrogen environment in the cell was kept during the experiment. The electrochemical measurements were carried out at an ambient temperature of $25 \pm 1\,^{\circ}C$.

The nitrogen gas adsorption/desorption isotherms at 77 K measured using a Micromeritics ASAP 2010 system. Ultraviolet–visible (UV–vis) absorption spectra were recorded with a Cary 50 Scan UV–vis spectrophotometer (Varian). A JASCO J-810 circular dichroism spectropolarimeter was used for CD spectral measurements using a quartz cell with a path length of 0.5 cm. The IR spectra (range: 4000–400 cm^{-1}, resolution: 2 cm^{-1}) were recorded with a Shimadzu 4200 FTIR spectrometer at $22 \pm 2\,^{\circ}C$.

2.3. Preparation of Cyt c/SBA-15 modified GC electrode

The GC electrode with 3-mm diameter was polished to a mirror-like finish with 0.3 and 0.05 μm alumina slurry. Subsequently, it was sonicated and washed with absolute alcohol and triple-distilled water successively, and then dried at room temperature.

Cyt *c* can be adsorbed readily onto SBA-15 through electrostatic interactions, especially in neutral buffer solution [15]. The Cyt *c* was absorbed on SBA-15 by stirring 8 mg molecular sieves in 0.12 mM Cyt *c* solution (pH 6.8 PBS) in a centrifuge tube for 2.5 h in an ice bath. Then the mixture were centrifuged, the supernatant was analyzed by UV–vis spectroscopy. The weakly adsorbed Cyt *c* onto the SBA-15 was removed by repeatedly washing with PBS solution (pH 6.8, 0.1 M) as above until there was no further detection of free Cyt *c* in the supernatant. A physical evidence for Cyt *c* loading was provided: SBA-15 undergoes a distinct color change from white to pink upon absorption of Cyt *c*. The entire blend in this research is handled by the same method, including measured characterizations.

The obtained suspension of 100 μl was then mixed with 5 μl of 5% Nafion to produce a mixed solution. 4 μl of the mixture were dropped onto the pretreated GC electrode surface, and dried at 4 °C for 4 h. The obtained electrode was also stored in refrigerator at 4 °C before use. In this study, the protein concentration and the ratio of proteins to SBA-15 were the same for both spectroscopic and electrochemical experiments.

3. Results and discussion

3.1. Spectroscopic analysis of Cyt c/SBA-15 system

3.1.1. Brunauer–Emmett–Teller (BET) method

Under the experimental conditions, nitrogen adsorption/desorption isotherms exhibit SBA-15 with a pore size of 6.8 nm, large enough to immobilize Cyt *c*. The pore size is reduced to 1.2 nm upon adsorption of Cyt *c*. The decrease indicates that the Cyt *c* molecules have successfully entered the pore channels of the thin film and immobilized on it.

3.1.2. UV–vis absorption spectroscopic characterization

The position of the Soret absorption band of iron heme provides information about conformation of heme proteins [24]. The UV–vis absorption spectrum of native Cyt *c* solution displayed a maximum absorption at 408 nm, while no absorption of opaque SBA-15 solution was observed (curves a and c in Fig. 1). Obviously, this absorption peak was attributed to the Soret band

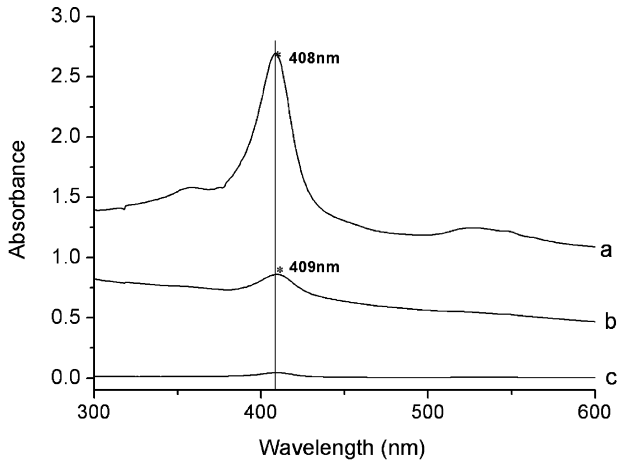

Fig. 1. UV–vis spectra of Cyt *c* (a) before, (b) after absorption onto SBA-15, 2.5 h stirring time and (c) SBA-15.

of Cyt *c*. For Cyt *c*/SBA-15 film, the absorption band was red shifted by only 1 nm at 409 nm (curve b in Fig. 1), the slight shift may be due to the interaction between SBA-15 and Cyt *c*. A shift of only 1 nm suggests that such interaction did not destroy the proteins' structure and the microenvironment of the proteins was slightly changed and no significant denaturation occurred.

3.1.3. Circular dichroism spectra characterization

As protein structures are dynamic and susceptible to operational conditions and environment, the integrity of the proteins was monitored by circular dichroism (CD) spectra in far-UV region (205–260 nm), which allows to evaluate the secondary structure in terms of β-sheet, α-helix and unordered forms of the polypeptide chain [25]. The noise of the Cyt *c* adsorbed on SBA-15 is very large owing to the blend is not transparent, resulting in the curve fluctuate intensively. However, the trend of the two spectra are very similar and exhibit CD intensity at 222 and 206–208 nm that are associated to a corresponding augmentation of α-helix structure, indicating that α-helix conformation is predominant in both of two conditions, although a feeble increase of the CD absorption at 208 nm in curve b in Fig. 2. Further analysis of these spectral data using Yang's model revealed no significant change in the α-helicity, suggesting that the secondary structure of the proteins remained intact during the course of immobilization [26]. On the other hand, SBA-15 does not affect the secondary structure of α-helix, as shown in Fig. 2.

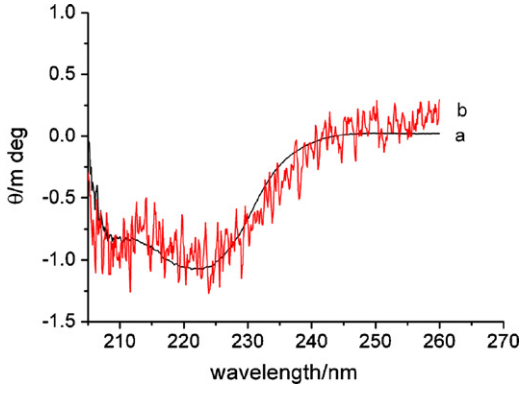

Fig. 2. Circular dichroism spectra of Cyt *c* (a) before and (b) after absorption onto SBA-15, 2.5 h stirring time.

3.1.4. FTIR spectra characterization

FTIR spectroscopy is a sensitive probe for secondary structure of proteins. If protein is denatured, the intensity of the characteristic bands will significantly weaken or even disappear [27]. As shown in Fig. 3a and c, the characteristic amide I (1700–1600 cm^{-1}) and amide II (1620–1500 cm^{-1}) bands of Cyt *c* entrapped in SBA-15 are nearly the same as those obtained in the protein spectrum. The similarity of spectra in Fig. 3 suggests that Cyt *c* retains the essential features of its original structure in the SBA-15 film.

3.2. The optimum orientation of Cyt c adsorption on the SBA-15

Owing to the p*I* of 10.6, Cyt *c* shows positive electricity in the neutral solution. The charges distribute asymmetrically on the surface, the amino acid residues with the positive charges are distributed on one end near the active area of the Cyt *c* molecule [28].

The special structure of Cyt *c* molecule with a flat plane exposing the heme group [21] means that there is only one electroactive position when the Cyt *c* molecule attaches to the surface. At the end of the attachment reaction all oriented molecules are taken up at an exclusive orientation, which benefits the electron transfer. Former research showed that the negative charge can promote the attachment of Cyt *c* in an orientation favorable for electron transfer [21]. The surface charges of the Cyt *c* and SBA-15 are complementary due to SBA-15 visualizes negative electricity in the neutral solution [15]. Therefore, the protein will adopt a preferred orientation for DETT when binding to SBA-15 surface through the interaction of the positively charged lysine residues on the protein surface with the

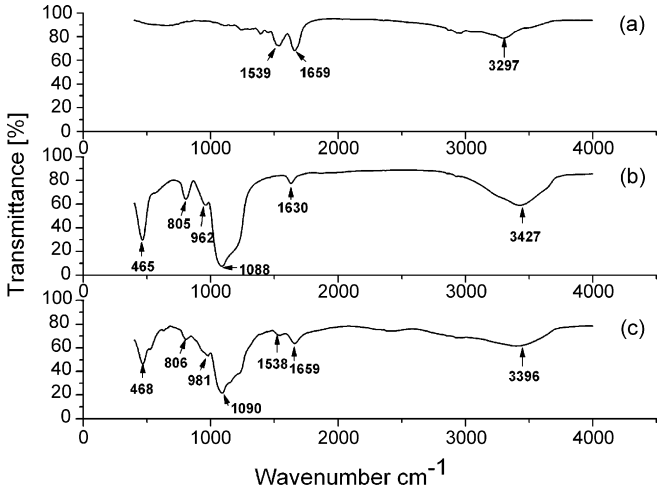

Fig. 3. FTIR spectra of (a) Cyt *c*, (b) SBA-15 and (c) Cyt *c* absorption onto SBA-15, 2.5 h stirring time.

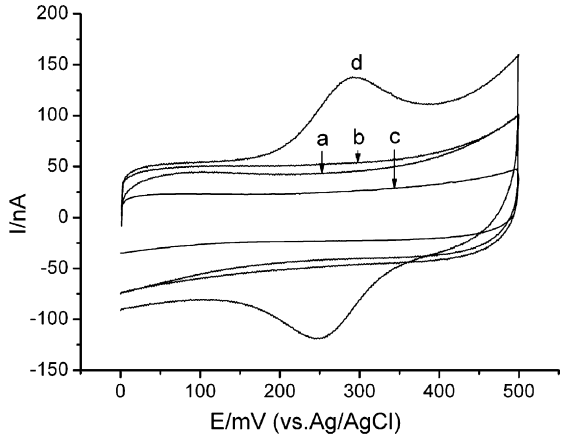

Fig. 4. Cyclic voltammograms of (a) GC electrode, GC electrode modified with (b) SBA-15, (c) Cyt *c*/Nafion and (d) Cyt *c*/SBA-15/Nafion in PBS (pH 6.8), scan rate 20 mV s^{-1}.

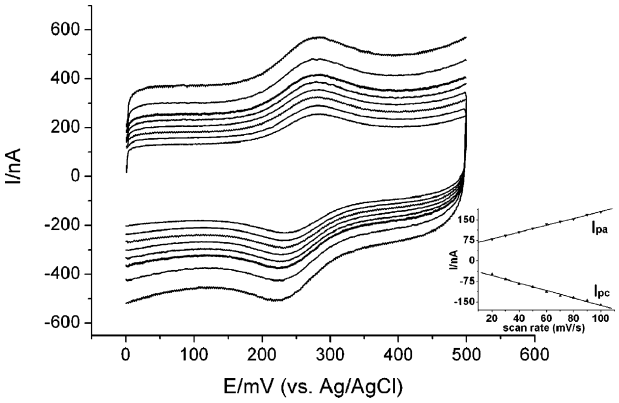

Fig. 5. Cyclic voltammograms of Cyt *c*/SBA-15/Nafion/GC electrode at various scan rates in PBS (pH 6.8), from inner to outer, the scan rates are 50, 60, 70, 80, 90, 100, 120 and 150 mV s^{-1}. The inset is the plot of anodic and cathodic peak currents vs. scan rate.

negatively charged silanol groups [4]. The optimal orientation may be determined by an unusual feature of the protein structure and brings about the slight change of the conformation, however, not destroying the structure and changing the fundamental microenvironment. The distance between the positive part of the dipole axis emerging from the protein near Ala-83 and the edge of the heme macrocycle (833CMC) can be as large as 0.97 nm [21].

3.3. Direct voltammetry of Cyt c on the glassy carbon electrode modified with SBA-15

As shown in Fig. 4, the bare GC electrode, the SBA-15 modified electrode and the Nafion/Cyt *c* modified electrode did not show any electrochemical response in curves a, b and c. Only the GC electrode covered with a Cyt *c*/SBA-15/Nafion film displayed a pair of well-defined quasi-reversible redox peaks as curve d. It demonstrated that SBA-15 played an important role in the direct electron transfer of Cyt *c*. The cyclic voltammograms (CVs) of immobilized Cyt *c* can also confirm that the protein retains activity and selectivity as usual upon immobilization [5]. The formal potential ($E^{0'}$) value of the modified electrode as 254 mV (vs. Ag/AgCl) is more positive than those of Cyt *c* immobilized in other analogous materials (shown in Table 1), the reason can be interpreted that the $E^{0'}$ values are sensitive to the conformation of the protein and the solvent medium [27]. A small change in the accessibility of the heme group to the protein exterior in solvents of different dielectric constants can modulate the heme reduction potential dramatically [29]. Cyt *c* on the modified electrode carries out a typical surface-controlled process [30] as shown in Fig. 5. The modified electrode was stable enough to retain its 90% electrochemistry activity when stored in a refrigerator at 4 °C for 15 days.

The electron-transfer rate constant κ_s was calculated according to the model of Laviron [31] with the fomula $\kappa_s = mnF\upsilon/RT$ to be 2.20 s^{-1}, where *m* is a parameter related to the peak-to-peak separation, indicating that the quasi-reversible reaction is a fast electron-transfer process. The calculated value was equal to the value for Cyt *c* entrapped in the nano-LTL-zeolite film [32], and larger than those of Cyt *c* and other heme-containing proteins immobilized in other mesoporous or sol–gel materials (Table 1). Thus, the host matrix of SBA-15 offers a suitable microenvironment for direct electron transfer between Cyt *c* and the electrode.

Using the integrals of the reduction peaks and Faraday's laws [30], $\Gamma^* = Q/nFA$, the amount of electroactive protein molecules was calculated to be 1.75×10^{-11} mol cm^{-2} for Cyt *c*, similar to that Cyt *c* immobilized in the agarose film 1.72×10^{-11} mol cm^{-2} [27], indicating a sub-monolayer of Cyt *c* on the modified GC [33]. Interestingly, the result makes it possible to educe that only 0.25% of the total amount of Cyt *c* deposited on the electrode surface present their activities. It is reasonable that only the 0.25% proteins in the inner layers of the films close to the electrode with a suitable orientation can exchange electrons fast with the electrode surface [27]. The number of electron exchange (*n*) could be calculated from the Langmuir film system as follows $i_p = nFQ\upsilon/4RT$. Therein, *n* could be 1.06, indicating the redox reaction of Cyt *c* on the SBA-15 belongs to a single electron-transfer process.

3.4. Electrocatalytic reduction of hydrogen peroxide on GC electrode modified with Cyt c/SBA-15

High-electrocatalytic activity had been exhibited in the CVs for the reduction of hydrogen peroxide on Cyt *c*/SBA-15/Nafion/GC electrode at different concentrations (Fig. 6). The cathodic peak current increased while the anodic peak current decreased dramatically. At the meanwhile, the reduction peak current increased with the increasing H_2O_2 concentration. Thus, the reduction of H_2O_2 on the modified electrode is a typical electrocatalytic reduction process.

Furthermore, the amperometric responses of the Cyt *c*/SBA-15/Nafion/GC electrode upon successive additions of H_2O_2 to 0.1 M pH 6.8 PBS at an applied potential of −0.2 V were shown in Fig. 7. As H_2O_2 was added into the stirring PBS, the biosensor responded rapidly to the substrate. The biosensor could achieve

Table 1
Electrochemical parameters of redox proteins on the different modified electrodes

Electrode	pH	$E^{0'}$ (mV) vs. Ag/AgCl	Ks (s^{-1})	Reference
Cyt *c*/SBA-15/GC	6.8	254	2.20	My work
Cyt *c*/nano-LTL-zeolite/ITO	7.0	59	2.20	[32]
Cyt *c*/agarose/GC	7.0	−522	0.70	[27]
Cyt *c*/Nafion/cysteine/gold	7.0	38	0.60	[34]
Cyt *c*/NaY/GC	7.0	0	0.69	[35]
Hb/HMS/GC	7.0	7	0.92	[36]

$E^{0'}$ and ΔEp were estimated as $(E_{pa} + E_{pc})/2$ and $(E_{pa} - E_{pc})$ in the CVs obtained with the modified electrodes in potassium phosphate buffer solution at 100 mV s^{-1}. E_{pa} and E_{pc} were anodic and cathodic peak potentials of the proteins, respectively.

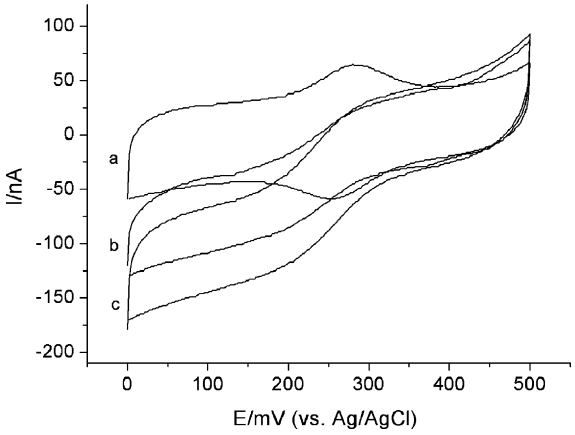

Fig. 6. Cyclic voltammograms of Cyt *c*/SBA-15/Nafion/GC electrode in 0.1 M pH 6.8 PBS (a) absence, (b) presence of 5 mM and (c) 10 mM H_2O_2, the scan rate is 20 mV s^{-1}.

95% of the steady-state current within 5 s, which indicates a fast diffusion process and a high activity of the Cyt *c* in this microelectrode system provided by SBA-15. The sensitivity of the proposed sensor was 17.5 μA mM^{-1} cm^{-2}, and the detection limit was estimated to be 2.1×10^{-8} M at 3σ. It can be seen that the interaction between Cyt *c* and SBA-15 plays an important role in direct electron-transfer behavior as well as high-electrocatalytic activity.

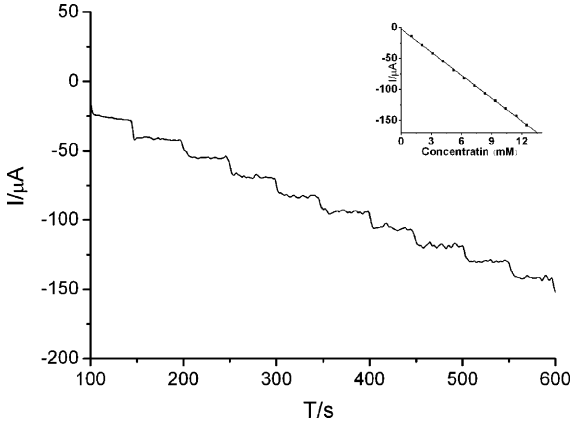

Fig. 7. Amperometric response of Cyt *c*/SBA-15/Nafion/GC electrode to H_2O_2, conditions −0.2 V constant potential, pH 6.8 and stirring speed is 2000 rpm: successive addition of 2 mM H_2O_2. Insets plot of chronoamperometric current vs. H_2O_2 concentration.

4. Conclusion

It was discovered that immobilizing Cyt *c* on SBA-15 could optimize electrochemistry microenvironment for the redox reaction of Cyt *c*. A dramatically high-cathodic redox potential was firstly observed from the Cyt *c*/SBA-15 system, in which the Cyt *c* kept its biological activity. In addition, both the electrochemical reversibility and electrocatalytic activity were enhanced by optimal DETT when binding to SBA-15 surface. A stable, quasi-reversible direct electrochemistry behavior of a surface-controlled electrode process with a single proton transfer had been obtained on the SBA-15 modified GC electrode. The optimal DETT is relative to a preferred orientation owing to the isoelectric point and static interaction when Cyt *c* immobilized on SBA-15, which permits easier access of the electron to the active sites of the redox protein. The present research provides a novel way to understand the essence of the electron transfer between protein and porous materials.

Acknowledgments

The authors are grateful for the financial sponsors: Nature Science Foundation of China (20433060), Foundation of State Key Laboratory of Electroanalytic Chemistry (2002003) and Foundation of State Key Laboratory of Physical Chemistry of Solid Surfaces (200407).

References

[1] D. Zhao, Q. Huo, J. Feng, B.F. Chmelka, G.D. Stucky, J. Am. Chem. Soc. 120 (1998) 6024–6036.
[2] Y.J. Han, J.M. Kim, G.D. Stuchy, Chem. Mater. 12 (2000) 2068–2069.
[3] L. Zheng, S. Zhang, L. Zhao, G. Zhu, X. Yang, G. Gao, S. Cao, J. Mol. Catal. B: Enzym. 38 (2006) 119–125.
[4] A. Salimi, E. Sharifi, A. Noorbakhah, S. Soltanian, Electrochem. Commun. 8 (2006) 1499–1508.
[5] L. Washmon-Kriel, V.L. Jimenez, K.J. Balkus Jr, J. Mol. Catal. B: Enzym. 10 (2000) 453–469.
[6] D.Y. Zhao, J.L. Feng, Q.S. Huo, N. Melosh, G.H. Fredrichson, B.F. Chmelka, G.D. Stuchy, Science 279 (1998) 548–552.
[7] Y. Wang, F. Caruso, Chem. Mater. 17 (2005) 953–961.
[8] J.M. Kisler, A. Dahler, G.W. Stevens, A.J. O'Connor, Micropor. Mesopor. Mater. 44/45 (2001) 769–774.
[9] J.M. Kisler, G.W. Stevens, A.J. O'Connor, Mater. Phys. Mech. 4 (2001) 89–93.
[10] H. Takahashi, B. Li, T. Sasaki, C. Miyazaki, T. Kajino, S. Inagaki, Chem. Mater. 12 (2000) 3301–3305.

[11] H.H.P. Yiu, C.H. Botting, N.P. Botting, P.A. Wright, Phys. Chem. Chem. Phys. (2001) 2983–2985.
[12] J.F. Diaz, K.F. Balkus Jr., J. Mol. Catal. B: Enzym. 2 (1996) 115–126.
[13] M.E. Gimon-Kinsel, V.L. Jimenez, L. Washmon, K.J. Balkus Jr., Stud. Surf. Sci. Catal. 117 (1998) 373–380.
[14] Y.S. Chaudhary, S.K. Manna, S. Mazumdar, D. Khushalani, Micropor. Mesopor. Mater. 109 (2008) 535–541.
[15] J. Deere, E. Magner, J.G. Wall, B.K. Hodnett, J. Phys. Chem. B 106 (2002) 7340–7347.
[16] J. Deere, E. Magner, J.G. Wall, B.K. Hodnett, Chem. Commun. (2001) 465–466.
[17] J. Deere, E. Magner, J.G. Wall, B.K. Hodnett, Catal. Lett. 85 (2003) 19–23.
[18] H.H.P. Yiu, P.A. Wrighyt, N.P. Botting, J. Mol. Catal. B: Enzym. 15 (2001) 81–92.
[19] A. Vinu, V. Murugesan, O. Tangermann, M. Hartmann, Chem. Mater. 16 (2004) 3056–3065.
[20] M. Hartmann, Chem. Mater. 17 (2005) 4577–4593.
[21] B.A. Kuznetsov, N.A. Byzova, G.P. Shumakovich, J. Electroanal. Chem. 371 (1994) 85–92.
[22] Y.M. Zhu, J.H. Li, S.J. Dong, Chem. Commun. (1996) 51–52.
[23] C. Yu, J. Fan, B. Tian, D. Zhao, Chem. Mater. 16 (2004) 889–898.
[24] P. George, G. Hanania, J. Biochem. 55 (1953) 236–243.
[25] M. Barteri, M.C. Gaudiano, S. Rotella, G. Benagiano, A. Pala, Biochim. Biophys. Acta 1479 (2000) 255–264.
[26] C.T. Chang, C.S. Wu, J.T. Yang, Anal. Biochem. 91 (1978) 13–16.
[27] S.F. Wang, T. Chen, Z.L. Zhang, X.C. Shen, Z.X. Lu, D.W. Pang, K.Y. Wong, Langmuir 21 (2005) 9260–9266.
[28] L. Zhu, D.M. Sun, T.H. Lu, C.X. Cai, C.P. Liu, W. Xing, Sci. China Ser. B: Chem. 50 (2007) 304–307.
[29] J.S. Vrettos, M.J. Reifler, K.V. Laksshmi, J.C. De paula, J. Biol. Inorg. Chem. 6 (2001) 708–716.
[30] A.J. Bard, Electroanalytical Chemistry, vol. 13, Marcel Dekker, New York, 1984.
[31] E. Laviron, J. Electroanal. Chem. 101 (1979) 19–28.
[32] T. Yu, Y.H. Zhang, C.P. You, J.H. Zhuang, B. Wang, B.H. Liu, Y.J. Kang, Y. Tang, Chem. Eur. J. 12 (2006) 1137–1143.
[33] X.L. Chen, N.F. Hu, Y.H. Zeng, J. Beijing Normal U 38 (2002) 515–520.
[34] J. Hong, H. Ghourchian, A.A. Moosavi-Movahedi, Electrochem. Commun. 8 (2006) 1572–1576.
[35] Z.H. Dai, S.Q. Liu, H.X. Ju, Electrochim. Acta 49 (2004) 2139–2144.
[36] Z.H. Dai, S.Q. Liu, H.X. Ju, H.Y. Chen, Biosens. Bioelectron. 19 (2004) 861–867.